Cinnamaldehyde accelerates wound healing by promoting angiogenesis via up-regulation of PI3K and MAPK signaling pathways

Article *in* Laboratory Investigation · February 2018

DOI: 10.1038/s41374-018-0025-8

CITATIONS
0

READS
24

13 authors, including:

Liwen Han
Shandong Academy of Sciences
23 PUBLICATIONS **53** CITATIONS

SEE PROFILE

Tai-Ping Fan
University of Cambridge
154 PUBLICATIONS **4,722** CITATIONS

SEE PROFILE

Laboratory Investigation
https://doi.org/10.1038/s41374-018-0025-8

ARTICLE

Cinnamaldehyde accelerates wound healing by promoting angiogenesis via up-regulation of PI3K and MAPK signaling pathways

Xing Yuan[1] · Lin Han[1] · Peng Fu[2] · Huawu Zeng[1] · Chao Lv[1] · Wanlin Chang[1] · R. Scott Runyon[3] · Momoko Ishii[3] · Liwen Han[4] · Kechun Liu[4] · Taiping Fan[3] · Weidong Zhang[1,5] · Runhui Liu[1]

Received: 2 May 2017 / Revised: 19 December 2017 / Accepted: 22 December 2017

Abstract

The bark of *Cinnamomum cassia* (*C. cassia*) has been used for the management of coronary heart disease (CHD) and diabetes mellitus. *C. cassia* may target the vasculature, as it stimulates angiogenesis, promotes blood circulation and wound healing. However, the active components and working mechanisms of *C. cassia* are not fully elucidated. The Shexiang Baoxin pill (SBP), which consists of seven medicinal materials, including *C. cassia* etc., is widely used as a traditional Chinese patent medicine for the treatment of CHD. Here, 22 single effective components of SBP were evaluated against the human umbilical vein endothelial cells (HUVECs). We demonstrated that in HUVECs, cinnamaldehyde (CA) stimulated proliferation, migration, and tube formation. CA also activated the phosphatidylinositol 3-kinase (PI3K) and mitogen-activated protein kinase (MAPK) pathways. Furthermore, the secretion of vascular endothelial growth factor (VEGF) from HUVECs was increased by CA. In vivo, CA partially restored intersegmental vessels in zebrafish pretreated with PTK787, which is a selective inhibitor for vascular endothelial growth factor receptor (VEGFR). CA also showed pro-angiogenic efficacy in the Matrigel plug assay. Additionally, CA attenuated wound sizes in a cutaneous wound model, and elevated VEGF protein and CD31-positive vascular density at the margin of these wounds. These results illustrate that CA accelerates wound healing by inducing angiogenesis in the wound area. The potential mechanism involves activation of the PI3K/AKT and MAPK signaling pathways. Such a small non-peptide molecule may have clinical applications for promoting therapeutic angiogenesis in chronic diabetic wounds and myocardial infarction.

Introduction

Impaired wound healing is a serious complication of diabetes that can result in chronic wounds and even amputation [1]. Chronic wounds represent a silent epidemic that affects a majority of diabetic patients and seriously diminishes their quality of life [2]. To decrease wound-related disorders, efficient wound management is essential. The process of repairing wounds requires a well-orchestrated integration of

These authors contributed equally: Xing Yuan, Lin Han.

Electronic supplementary material The online version of this article (https://doi.org/10.1038/s41374-018-0025-8) contains supplementary material, which is available to authorized users.

✉ Taiping Fan
tpf1000@cam.ac.uk

✉ Weidong Zhang
wdzhangy@hotmail.com

✉ Runhui Liu
lyliurh@126.com

[1] School of Pharmacy, Second Military Medical University, Shanghai 200433, P.R. China

[2] Department of Pharmacy, Changhai Hospital, Second Military Medical University, Shanghai 200433, P.R. China

[3] Department of Pharmacology, University of Cambridge, Cambridge CB2 1PD, UK

[4] Biology Institute, Shandong Academy of Sciences, Jinan 250014, P.R. China

[5] Institute of Interdisciplinary Research Complex, Shanghai University of Traditional Chinese Medicine, Shanghai 200040, P.R. China

Published online: 20 February 2018

complex biological and molecular events. Angiogenesis is a critical step in wound healing, which regenerates blood vessels and enables the oxygen supply that is necessary to stimulate repair and vessel growth [3]. It is well established that the MAPK and PI3K/AKT signaling pathways are involved in angiogenesis, and these pathways contribute to different stages of this process [4, 5]. The MAPK family is a large family of serine/threonine kinases, including three well-characterized subfamilies, Erk1/2, P38, and JNK/SAPK, which mediate a variety of cell functions, such as proliferation (Erk1/2) and migration (P38) [6, 7]. AKT, a general regulator in angiogenesis, likely contributes to endothelial cell survival and growth [8]. Although many angiogenic growth factors/cytokines have been shown to have clinical potential in wound healing, only recombinant human platelet-derived growth factor-BB (rhPDGF-BB; becaplermin) has been approved by the Food and Drug Administration (FDA) for topical use in diabetic neuropathic lower extremity ulcers [9]. However, the high cost and lack of alternative delivery mode limit the clinical application of PDGF [9, 10]. Significantly, the FDA has added a black box warning label about the risk of cancer, which is associated with the use of three or more tubes of Becaplermin [11]. Traditional medicinal herbs and pure compounds isolated from plants have been used for centuries for treating chronic wounds in Asia and Africa [12, 13]. Through years of trial and error, practitioners of alternative medicine have acquired a basic understanding of the safety and efficacy of medicinal herbs. Evidence-based confirmation in validated trials and investigations into the mechanisms of action that are responsible for the clinical effects of these herbs are of high clinical value. *Cinnamomum cassia* (*C. cassia*) is commonly used as a spice and flavoring agent and has been shown to be safe when ingested [14]. The bark of *C. cassia* has also been approved as a herbal medicine by the Chinese Pharmacopoeia as an analgesic and for promoting blood circulation [15]. There is a mounting evidence that *C. cassia* has anti-oxidative, antimicrobial, anti-cardiovascular disorders [16, 17], and antidiabetic effects [18–20]. Kamath et al. [21] and Farahpour et al. [22] found that an ethanol extract of *C. cassia* improved wound healing due to its anti-oxidant and antimicrobial properties. In addition, *C. cassia* stimulates angiogenesis in vivo and in vitro by up-regulating vascular endothelial growth factor (VEGF) and Flk-1/KDR expression [23]. However, the components of *C. cassia* that are mainly responsible for these pharmacological actions have not been fully characterized.

Shexiang Baoxin Pill (SBP), which is a well-known traditional Chinese patent medicine, comprises seven medicinal materials including *C. cassia*. It is commonly used in the treatment of coronary heart disease (CHD) [24–26]. Cinnamaldehyde (CA) is an essential oil isolated from the bark of *C. cassia* [27]. In the present study, CA was found to have pro-angiogenic properties against human umbilical vein endothelial cells (HUVECs). Therefore, we aimed to evaluate the pro-angiogenic effects of CA including the promotion of cell proliferation, migration, and tube formation of HUVECs. We also tested the ability of CA to promote angiogenesis and enhance wound healing in animal models.

Materials and methods

Materials

CA (purity>99.0%) was purchased from the Beijing Naturally Occurring Drugs Research Institute, China. A stock solution of CA was prepared in dimethyl sulfoxide (DMSO) at 10 mM and stored at −20 °C until use. Cell Counting Kit-8 (CCK-8) was from Dojindo Molecular Technologies (Kumamoto, Japan). CFDA-SE Cell Proliferation Assay and Tracking Kit was purchased from Beyotime Institute of Biotechnology (Jiangshu, China). VEGF, sodium heparin, Hochest 33258, and PTK787 were from Sigma (St. Louis, MO). Growth factor reduced Matrigel; Annexin V-FITC/PI Apoptosis Detection Kit was from BD Biosciences (San Jose, CA, USA). Specific rabbit polyclonal antibodies to endothelial nitric oxide synthase (eNOS), phospho-eNOS (Ser1177), AKT, phospho-AKT (Ser473), p38, phospho-p38 (Thr180/Tyr182), c-Raf, phospho-c-Raf (Ser338), Erk1/2, phospho-Erk1/2 (Thr202/Tyr204) and β-actin (as a loading control), U0126 (a MEK inhibitor), and LY294002 (a PI3K inhibitor) were from Cell Signaling Technology (Danvers, MA, USA). A hemoglobin human ELISA kit and monoclonal antibodies against VEGF and CD31 were from Abcam (Cambridge, UK). A human VEGF ELISA Kit was from eBioscience (San Diego, CA). All of the other chemicals were from Invitrogen (Carlsbad, CA) or otherwise indicated.

Cell culture and animal maintenance

Primary HUVECs were purchased from AllCells (Emeryville, CA, USA). With the exception of the homocysteine-rescue tube assay, each batch of HUVECs was examined using flow cytometry and was shown to be 99% CD31 positive, with a viability of 95%. Unless otherwise indicated below, cells were cultured in MCDB131 medium supplemented with EGF, bFGF, cAMP, heparin, hydrocortisone, penicillin, streptomycin, amphotericin B, and 10% fetal bovine serum (FBS) on 25 cm CellBIND® flaks (Corning®, USA) at 37 °C, 5% CO_2. HUVECs from passages 2 to 6 were used for experiments. Human dermal fibroblasts (HDFs) were obtained from foreskin samples from

circumcisions, and were a gift from Dr. William English, Cancer Research UK Cambridge Research Institute in Cambridge, UK. HDFs were grown in Dulbecco's modified Eagle's Medium, 10% FBS, and ANTI-ANTI.

Male diabetic (BSK.Cg-m+/+Lepr^{db}; *db/db*) and WT mice (C57BL/6J), and male Kunming mice were all obtained from the Shanghai SLAC Laboratory Animal Co., Ltd. (Shanghai, China). The animals were maintained under specific pathogen-free conditions with food and water supplied ad libitum in the Laboratory Animal Center of the Second Military Medical University. All animal experiments were carried out in accordance with the Guide for the Care and Use of Laboratory Animals of the National Institutes of Health and were approved by the Committee on the Ethics of Animal Experiments of the Second Military Medical University, China.

Cell proliferation assay

Cell viability was measured by the Cell Counting Kit-8 (Dojindo, Kumamoto, Japan) according to the manufacturer's instruction. HUVECs (5×10^3 cells, 100 μL per well) with 10% FBS culture medium were seeded in 96-well plates. After attachment, the medium was replaced with MCDB131 containing 1% FBS, and then the growth medium was supplemented with different bioactive components (10 μM) from SBP and varying concentrations of CA (0.1, 0.5, 1, 5 and 10 μM). VEGF (20 ng/mL) was added as the positive control and no supplemented compounds and VEGF were added as the blank control. After incubation as indicated time, the number of viable cells was determined by the CCK-8 assay according to the manufacturer's protocol. Briefly, the CCK-8 solution was added to each well and incubated at 37 °C in humidified 95% air and 5% CO_2 for a further 3 h. The absorbance was measured at 450 nm for each well using a Microplate Reader (Bio-Rad, Hercules, CA). Carboxyfluorescein diacetate, succinimidyl ester (CFSE) analysis was further performed to track HUVEC division using a CFDA-SE Cell Proliferation Assay and Tracking Kit (Beyotime Biotech), and analyzed using flow cytometry (FACS Calibur).

Cell apoptosis assay

HUVECs were seeded in six-well plates (3×10^5 cells per well) for 24 h and then treated with CA (10 μM) or 1% DMSO (as control). After 24 h, the cells floating in the medium were collected, and the adherent cells were detached with 0.05% trypsin, washed twice with cold phosphate-buffered saline (PBS), and centrifuged at 1000 rpm for 5 min at 4 °C. Subsequently, HUVECs were gently resuspended in the binding buffer. Thereafter, the cells were stained using the Annexin V-FITC/PI apoptosis detection kit. After incubation at room temperature for 15 min in the dark, the apoptotic cells were immediately analyzed by flow cytometry (FACS Calibur).

Endothelial healing assay

HUVECs (1.5×10^5 cells per well) were seeded onto 12-well plates containing a plastic coverslip (Thermanox; Lux Scientific Corp., Newbury Park, CA) in each well which was coated with 0.5% gelatin. On reaching confluence, the coverslips were removed to leave a sharp wounded margin. Cells were incubated for 24 h in the presence or absence of CA (0.1, 0.5, 1, and 10 μM) in basal medium containing 1% FBS, after which they were harvested and counted by a hemocytometer. To further illustrate the effect of CA in stimulating endothelial wound healing, a scratch assay was performed. HUVECs (3×10^4 cells, 400 μL per well) were plated in 0.5% gelatin pre-coated 24-well plates in regular growth medium. After attachment, a rectangular wound was scratched in the center of the cell monolayer using a 200 μL sterile plastic pipette tip. The wounded monolayer was rinsed with PBS and then incubated with basal medium containing 1% FBS with various concentrations of CA (0.1, 0.5, 1, and 10 μM) for 24 h. Images of the wounds were recorded in five random fields (×100) with a phase-contrast microscope (Leica DMI3000 B, Wetzlar, Germany) before and after treatment. Distance was measured using Image J (National Institutes of Health, Digital Equipment Corp). The wound healing ability was quantified by the formula as followed:

$$\text{Ratio of wound healing}\% = 100\% - \frac{\text{Width 24h}}{\text{Width 0h}} \times 100\%.$$

Cell migration assay

The migration assay was performed using 24-well Boyden chamber transwells with porosity polycarbonate membrane inserts (8 μm pore size; Costar, Corning, NY, USA). In brief, HUVECs (5×10^4 cells per well) were suspended in basal medium (100 μL) in the presence or absence of CA (0.1, 1, 5, and 10 μM) for 30 min, and then seeded in the upper compartment of the chamber. The lower chamber was filled with 600 μL basal medium supplemented with 20% FBS and VEGF (20 ng/mL). After a 24 h incubation at 37 °C and 5% CO_2, the non-migrated cells were scraped off, and the cells that migrated across the filter were washed with PBS twice and stained with Hochest 33258 (10 μg/mL) for 10 min at room temperature. Stained cells were fixed with 4% paraformaldehyde and photographed using a fluorescent inverted microscope (×40) in five random high power fields (HPF). Finally, the migrated cells were counted

with Image-Pro Plus software (version 6.0, Media Cybernetics, Silver Spring, MD, USA) in triplicate.

Tube formation assays

Growth factor reduced Matrigel (BD, Bedford, MA, USA) was added to a 96-well plate (50 μL per well) and polymerized for 30 min at 37 °C. HUVECs (5×10^4 cells, 100 μL per well) were seeded into the coated plate in MCDB131 containing 1% FBS with or without CA (0.1, 1, 5, and 10 μM) and with VEGF (20 ng/mL) as a positive control. After 4 h, images were captured with an inverted microscope (×40) in five random fields. The number of tube-like structures per field was counted in a blinded manner and compared with control. The homocysteine-rescue tube formation assay was based in part on the co-culture model. Briefly, HUVECs and HDFs were seeded at a 1:20 ratio, or around 500 HUVECs to 10^4 HDFs per well in a 96-well flat-bottom plate in EGM-2 (Lonza). After 4 days, EGM-2 was titrated with its basal medium (EBM-2) and 2% FBS, and homocysteine and VEGF or CA were added and replenished every two days before staining on day 12. Cells were then fixed using 4% paraformaldehyde, permeabilized, and stained with an anti-human-von Willebrand Factor monoclonal antibody (Sigma) and an anti-rabbit alkaline phosphatase-conjugated secondary antibody. Tubes were visualized using the 1-Step™ NBT/BCIP, images were taken at ×40, and average tube size was measured using Image J.

Enzyme-linked immunosorbent assay

The concentration of VEGF in conditioned medium was determined using enzyme-linked immunosorbent assay (ELISA). In brief, HUVECs (3×10^4 cells per well) were cultured in 24-well plates in a volume of 300 μL. After attachment, cells were treated with different concentrations of CA (1, 5, and 10 μM) for the indicated time (24, 36, 48, and 72 h). The VEGF levels in the supernatants were determined as described by the manufacturer's instructions.

Western blot assay

2×10^5 cells were seeded into a six-well cell-binding plate (Corning) and then exposed to test medium for different times. Cells were washed with ice-cold PBS and lysed in RIPA buffer (150 mM NaCl, 50 mM Tris, pH 8.0, 0.02% NaN_3, 0.2% Aprotinin, 1% Triton X-100) supplemented with 1 mM phenylmethylsulfonyl fluoride and protease inhibitor cocktail (Thermo Scientific). Equal amounts of protein were separated on 10% sodium dodecyl sulfate polyacrylamide gel electrophoresis gels and subsequently transferred to polyvinylidene fluoride membranes. After blocking, the membranes were incubated with primary antibodies against target proteins overnight at 4 °C, followed by incubation with a secondary antibody (IRDye 800; LI-COR, Biosciences). Proteins in the blots were visualized using the Odyssey Infrared Imaging System (Li-COR Bioscience, Lincoln, NE, USA).

Zebrafish assays

The transgenic zebrafish strain, Tg (vegfr2: GFP), was maintained in the Children's Hospital breeding colony at 28.5 °C on a 14 h light/10 h dark cycle. Zebrafish embryos were generated by natural pair-wise mating (3–12 months old) and were raised at 28 °C in culture water (containing 5.0 mM NaCl, 0.17 mM KCl, 0.4 mM $CaCl_2$, 0.16 mM $MgSO_4$). Healthy, hatched zebrafish embryos were picked out at 21 h post-fertilization (hpf) and distributed into 24-well microplates (6–8 embryos per well). The zebrafish embryos were first treated with VEGFR inhibitor PTK787 (CAS: 212141-51-0, Sigma) from the concentration 0.5 to 3 μg/mL for 3 h to evaluate the tolerance dose. Then they were pretreated with 2.0 μg/mL PTK787 for 3 h, PTK787 was subsequently washed out and replaced with either 0.25% DMSO (v/v) in culture water (vehicle control), or increasing concentrations of CA of 0.01, 0.05, 0.1 μg/mL for 24 h. Each experiment was repeated at least three times.

Matrigel plug angiogenesis assay in vivo

Effect of CA on VEGF-stimulated angiogenesis in vivo was determined by Matrigel plug implantation assay which was based on the method of Wake et al. [28]. Briefly, the 5-week-old male Kunming mice (25–28 g) were subcutaneously injected with 0.5 mL of liquid Matrigel (BD Bioscience) mixture containing 100 ng/mL VEGF and 100 units/mL heparin. Then the mice were treated daily for 2 weeks with intraperitoneal injections of either vehicle (4% tween-80 in saline) or CA (100 mg/kg in the vehicle). After the 15th day, the mice were euthanized, and the Matrigel plugs were excised and photographed. Then a portion of Matrigel plugs was homogenized in PBS (pH 7.4) and centrifuged at 10,000 rpm for 10 min. The concentration of Hb in the supernatant was measured at 450 nm directly using a hemoglobin human ELISA kit (Abcam).

Wound healing in vivo

The male diabetic (BSK.Cg-m+/+Lepr^{db}; *db/db*) and WT mice (C57BL/6J) were 10 weeks old at the beginning of the experiments; *db/db* mice weighed 55–60 g with average blood glucose levels of 26.8 ± 0.6 mmol/L and WT mice weighed 20–25 g with average blood glucose levels of 6.1 ± 0.4 mmol/L. The skin wound study was performed as previously described [29]. Briefly, after shaving the chosen area

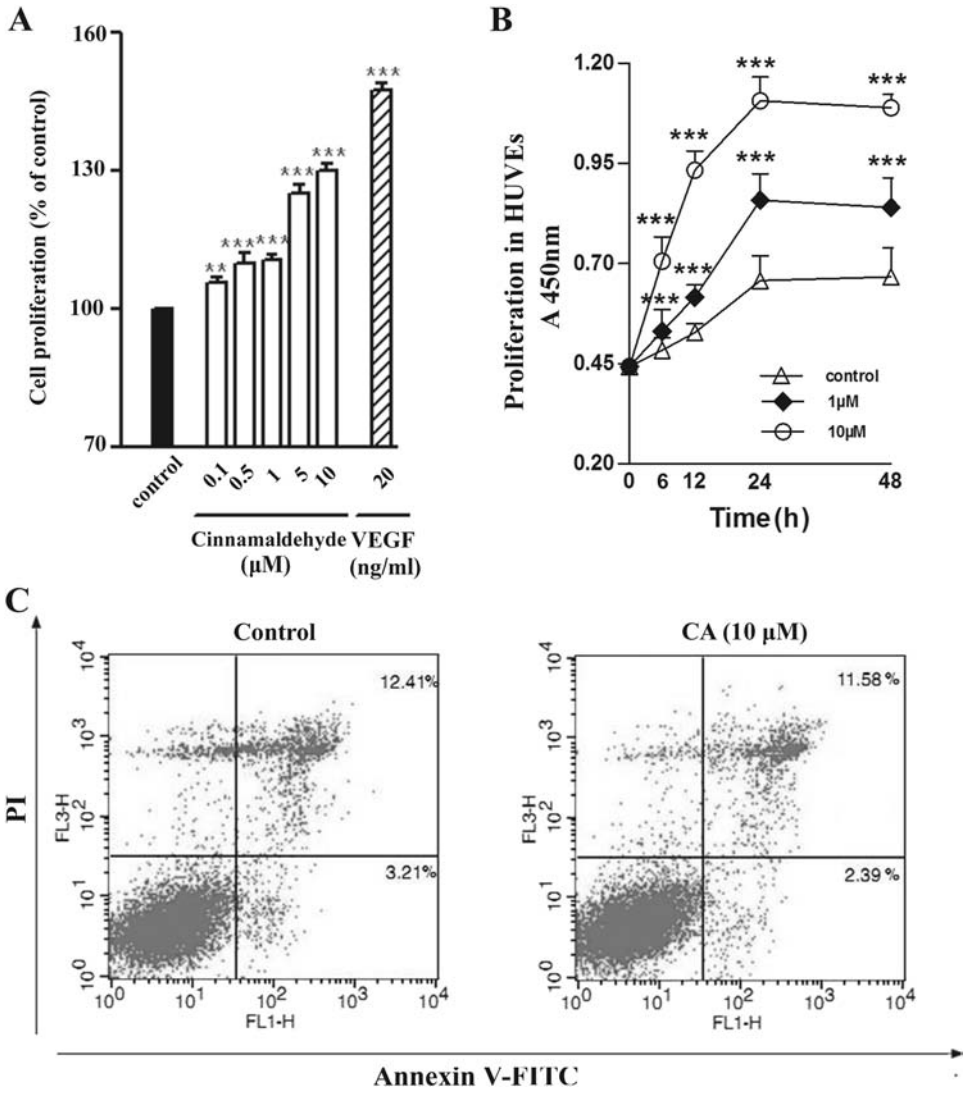

Fig. 1 Effects of cinnamaldehyde (CA) on human umbilical vein endothelial cells (HUVECs) proliferation and apoptosis. **a**, **b** The concentration- and time-dependent effects of CA on cell proliferation were determined using the CCK-8 assay. Cells were incubated with increasing concentrations of CA (0.1–10 μM) and VEGF (20 ng/mL) for 24 h (**a**). Cells were treated with CA at 1 and 10 μM for the indicated time (**b**). **c** HUVECs were stained with Annexin V-FITC and propidium iodide (PI) after the treatment with CA (10 μM) for 24 h. Percentages represent Annexin V-positive/PI-negative (early stage of apoptosis, lower right quadrant) and Annexin V-positive/PI-positive cells (later stage of apoptosis, upper right quadrant). Experiments were conducted from three individual experiments ($n = 3$ per experiment). Data shown in the graphs are representative of the mean ± SEM. $^{**}P < 0.01$, $^{***}P < 0.001$ vs. vehicle control

of the dorsal surface under anesthesia, a circular full-thickness excisional skin wound of 8-mm diameter was created using a surgical punch. Wounded mice ($n = 10$/each group) were randomly divided into three (WT group) or four (*db/db* group) groups and given an intraperitoneal injection with various concentrations of CA (WT group: 25, 50 mg/kg; *db/db* group: 25, 50, and 100 mg/kg) or vehicle solution every day. The wounds were photographed daily and diameters were calculated using Vernier callipers at the widest point of the wound. The change in wound size was expressed as wound closure, calculated using the formula as follows:

$$\text{Wound closure}\% = \frac{\text{wound diameter on day 0} - \text{wound diameter on day indicated}}{\text{wound diameter on day 0}} \times 100\%.$$

Five mice randomly chosen from each group were sacrificed. The cutaneous wound edges were harvested and divided into two parts, one for western blot assay and the other for histological analysis.

Histology and immunohistochemistry

To further investigate the potential angiogenic effect of CA in vivo, the HE staining and CD31 immunostaining analysis was performed on the remaining Matrigel plugs and cutaneous wound edges. Briefly, the Matrigel plugs and the skin from the healed wound beds surrounded by a margin of normal skin were harvested separately and were fixed in a 10% formalin solution, processed, embedded, sectioned, and either HE stained or IHC stained using antibodies against CD31. The HE and IHC images were obtained on a Leica DMI3000 B phase-contrast microscopy. The

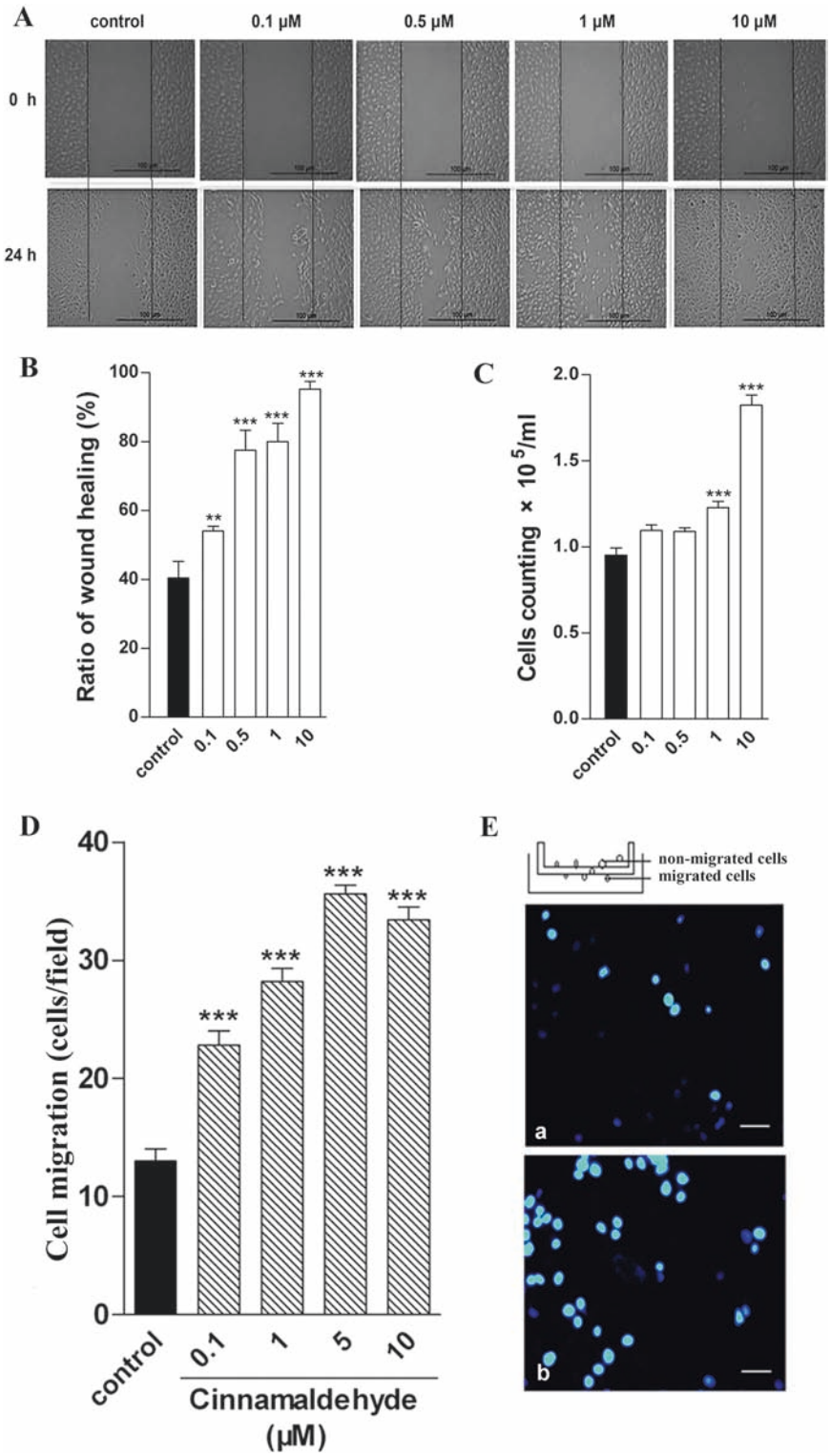

Fig. 2 CA induced endothelial cell wound healing and migration. **a**, **b** HUVEC wounds were created and then treated with CA at 0.1–10 μM for 24 h. The images were obtained at the same positions at time 0 h and after 24 h treatment with CA (**a**). Wound healing was evaluated by measuring the distance between the wound margins (**b**). **c** HUVECs (1.5×10^5 cells per well) were seeded onto a 12-well plate that contained plastic coverslips, and the wounded cells were treated with CA (0.1–10 μM) after removing the coverslips. After the 24-h incubation, the number of cells in each well was counted. **d**, **e** HUVECs were seeded into the upper chamber of a transwell plate at a density of 5×10^4 cells per well and then incubated with various concentrations of CA (0.1–10 μM). After 24 h, the migrated cells were quantified via manual counting (**d**) and photographed (**e**) with a fluorescent inverted microscope (magnification ×40). **e** Representative photographs of the cells that migrated across the membrane: **a** control; **b** CA (10 μM). Three individual experiments were conducted in triplicate. Data that are shown in the graphs are representative of the mean ± SEM. $^{**}P < 0.01$, $^{***}P < 0.001$ vs. the control

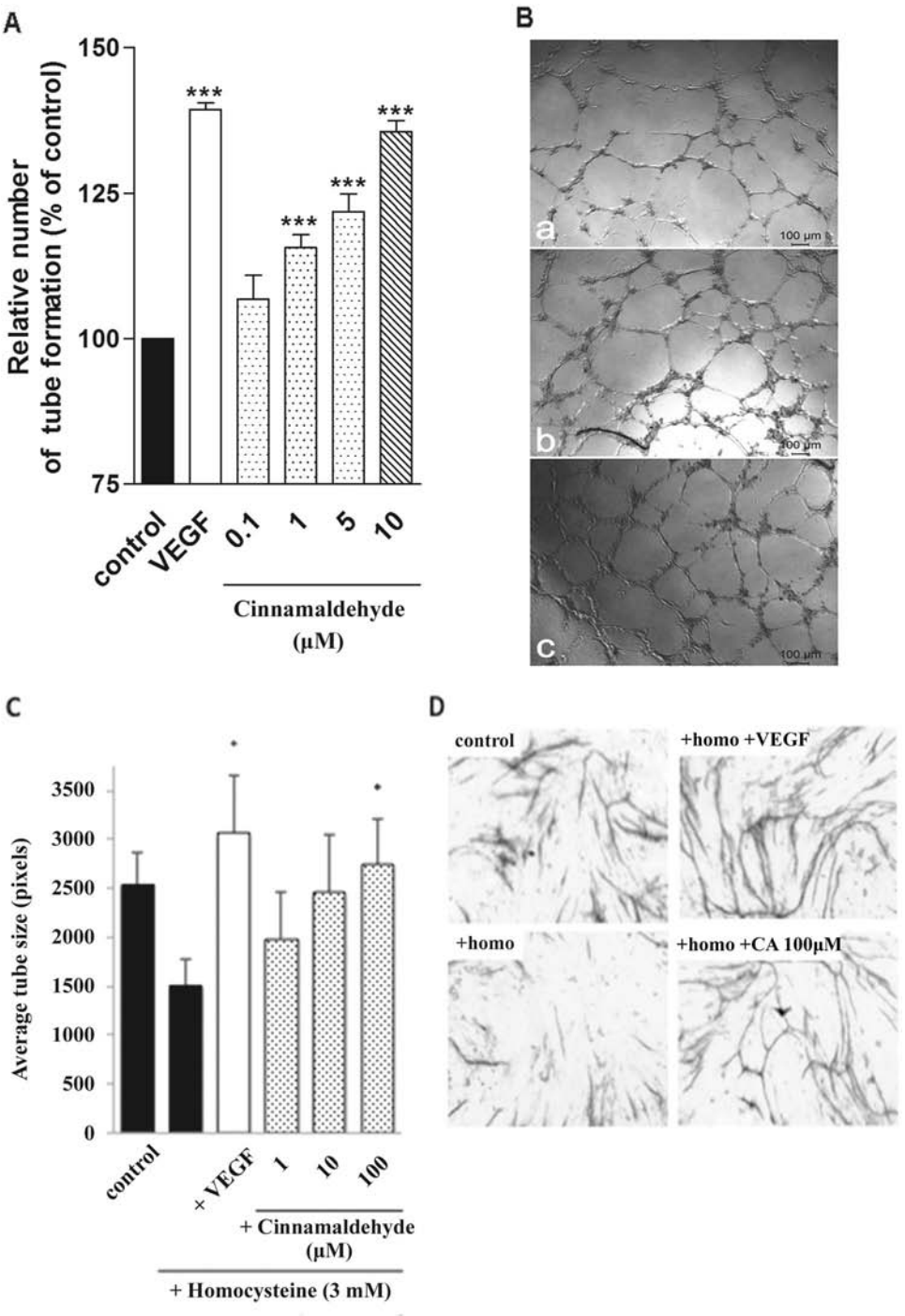

Fig. 3 CA enhanced endothelial cell tube formation in HUVECs. **a** HUVECs (5×10^4 cells per well) were plated in growth factor reduced matrigel-coated 96-well plates and then supplemented with or without various concentrations of CA (0.1–10 μM) for 4 h. The number of tube-like structures was calculated and expressed as the relative number of tube formation. **b** Representative photographs of the tube-like structures: **a** control; **b** CA (10 μM); **c** VEGF (20 ng/mL) (magnification ×40). **c** HUVECs (5×10^3 cells per well) and HDFs (1×10^5 cells per well) were plated and then challenged after 4 days with homocysteine with or without varying concentrations of CA (1–100 μM) over 8 days. Average tube size was calculated and expressed relative to the VEGF (20 ng/mL) rescue. Two images were taken and averaged per well for $n = 3$ wells per condition and compared using the *T*-test, $^{*}P < 0.05$ vs. the homocysteine alone (second row). **d** Photographs of the tubes. Data that are shown in the graphs are representative of the mean ± SEM. $^{*}P < 0.05$, $^{***}P < 0.001$ vs. the control

immunoreactive areas in the IHC images were quantified using Image J. The integrated optical density values were represented as the mean ± SEM.

Statistical analysis

One-way analysis of variance followed by Dunnet's correction was used to compare the significant differences between groups and *t*-test was used when two groups are compared. All quantitative data are expressed as the mean ± SEM. *P*-values less than 0.05 were considered significant.

Results

CA stimulated HUVEC proliferation

Aimed at discovering potential pro-angiogenic agents of SBP, CA, and other 21 compounds, single doses of 10 μM

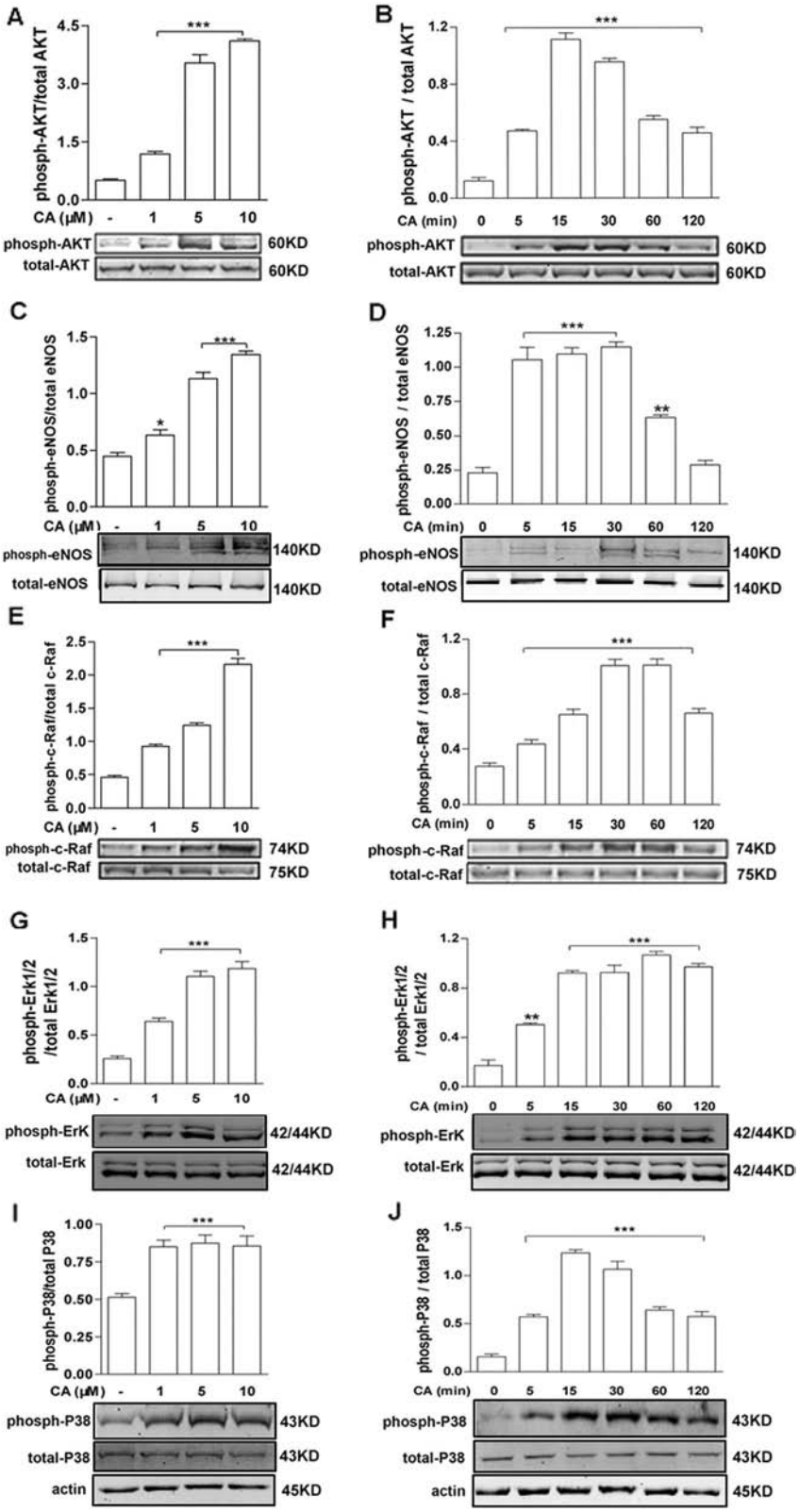

Fig. 4 CA activated the PI3K/AKT and MAPK signaling pathways. The effects of varying concentration (1–10 μM CA for 30 min) and time (10 μM CA for 0–120 min) of CA were determined via the western blot assay. Phosphorylation of AKT (**a**, **b**), eNOS (**c**, **d**), c-Raf (**e, f**), Erk1/2 (**g**, **h**), and p38 (**I**, **j**) in HUVECs stimulated with CA were measured. The representative images are from three individual experiments. Data shown in the graphs are representative of the mean ± SEM. $^{***}P < 0.001$, $^{**}P < 0.01$, $^{*}P < 0.05$ vs. the control

were employed in the preliminary screen to identify pro-angiogenic activity against the HUVECs. VEGF was used as a positive control at 20 ng/mL. Compared with the vehicle (DMSO) control, CA showed the most potent stimulation for endothelial cell proliferation (Supplementary Table S1); therefore, CA was evaluated further. The effect

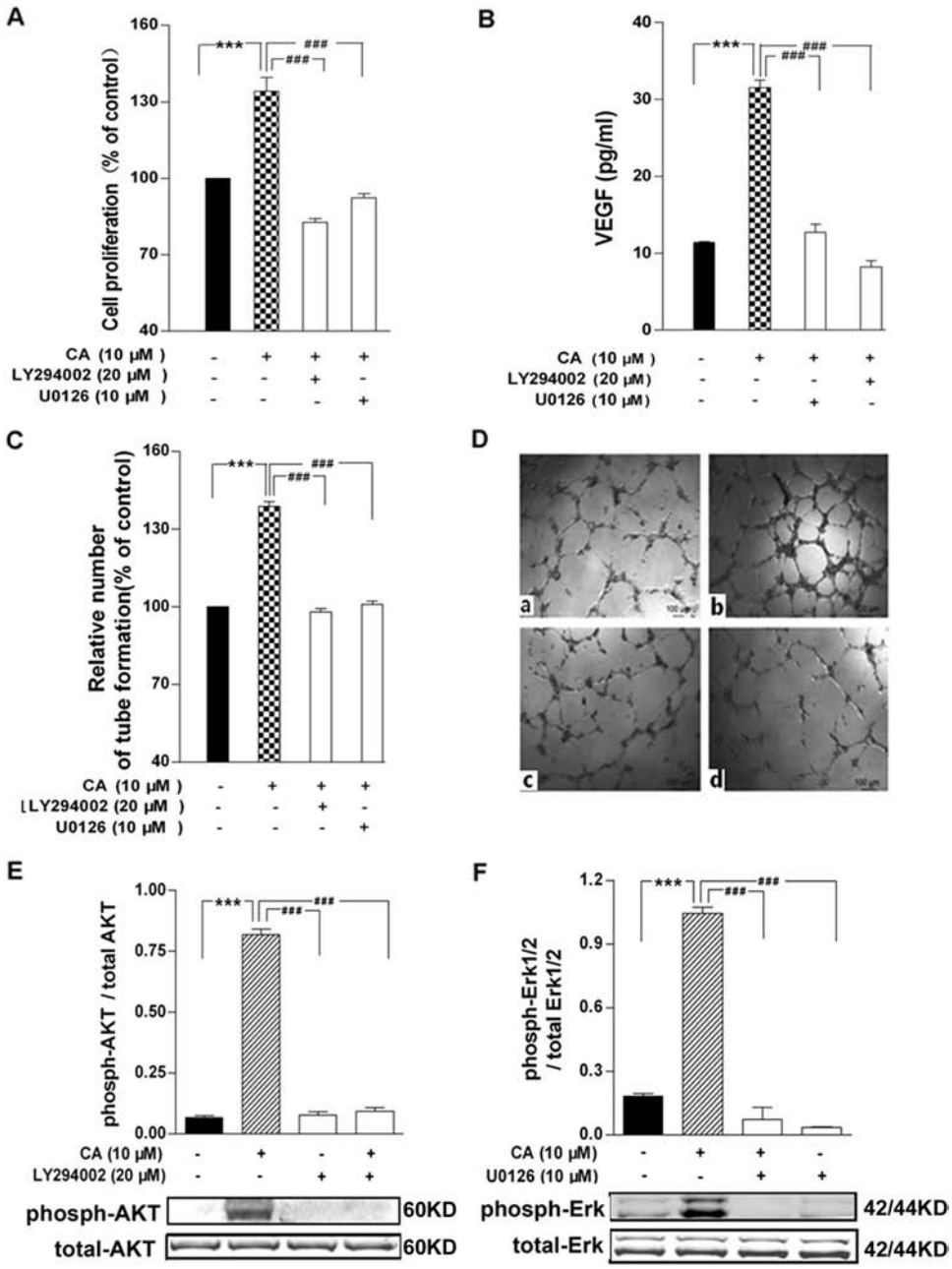

Fig. 5 Angiogenic activity of CA was responsible for the PI3K/AKT and MAPK signaling pathways. **a** Cell proliferation was measured in HUVECs that were treated with 10 μM CA for 24 h after pre-incubation with LY294002 (a PI3K inhibitor, 20 μM) or U0126 (a MEK inhibitor, 10 μM) for 30 min). **b** The secretion of VEGF was evaluated using ELISA in HUVECs stimulated with 10 μM CA for 48 h after pretreatment with LY294002 or U0126 for 30 min. **c** Tube formation was measured in HUVECs stimulated with 10 μM CA for 4 h and after pretreatment with LY294002 or U0126 for 30 min. **d** Representative photographs of tube-like structures: **a** control; **b** CA; **c** CA+ LY294002; **d** CA+ U0126. **e**, **f** HUVECs were pretreated with LY294002 (**e**) or U0126 (**f**) before the exposure to CA (10 μM). After a 30-min incubation, the levels of phosphorylated and total AKT or Erk1/2 were detected using a western blot. Experiments were conducted in triplicate. Data shown in the graphs are representative of the mean ± SEM. $^{***}P < 0.001$ vs. the control, $^{###}P < 0.001$ vs. CA

of CA on endothelial cell proliferation, an important early aspect of angiogenesis, is shown in Fig. 1a, b and Supplementary Figure S1. Using the CCK-8 assay, medium absorbance from the CA-treated cells was compared to that from vehicle control, and expressed as a percentage. CA significantly increased proliferation of HUVECs in a concentration- and time-dependent manner. The maximal increase of cell proliferation by CA (31.6% vs. the control) was achieved at 10 μM after 24 h. M1 represents the percentage of undivided cells in Supplementary Figure S1; the CFSE result showed the potent stimulation for endothelial cell proliferation by CA at 10 μM. In addition, 10 μM CA had no acute cytotoxic effects on HUVECs when cell apoptosis was detected by flow cytometry (Fig. 1c).

CA induced HUVEC wound closure

To evaluate the effect of CA on endothelial cell wound healing in vitro, the distance between the wound margins and the number of impaired HUVECs in the culture was determined. As Fig. 2a, b showed, at a lower concentration (0.1 μM), CA caused significantly larger wound closure (54.1 ± 2.8%) compared with the control (40.4 ± 8.3%) at 24 h. Treatment with 0.5 and 1 μM CA extensively

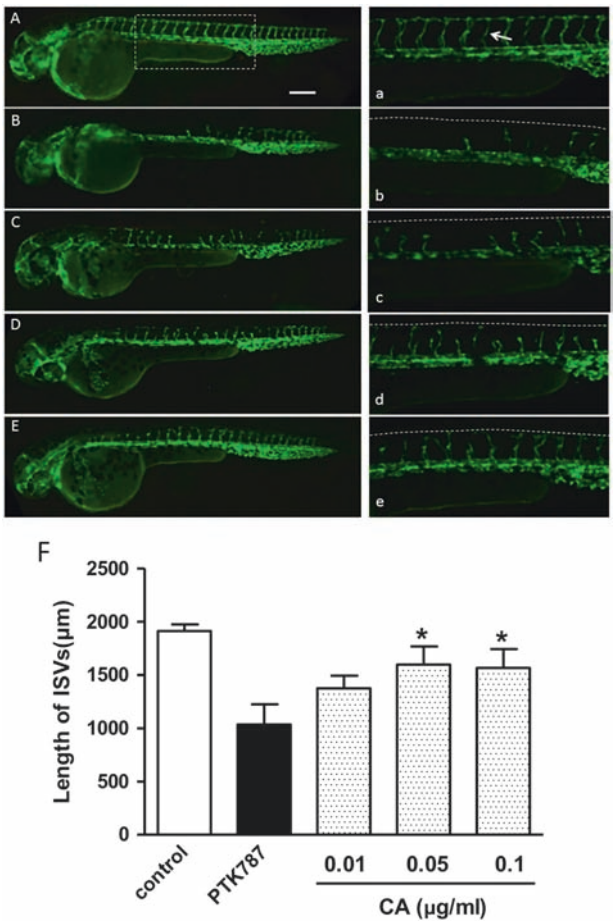

Fig. 6 Effects of CA on PTK787-induced intersegmental vessel loss in Tg (vegfr2: GFP) zebrafish. **a** Normal 48 hpf zebrafish. **b** Zebrafish was treated with PTK787 (2.0 μg/mL). **c**–**e** Zebrafish was treated with 0.01–0.1 μg/mL of CA for 24 h after pretreatment with PTK787 (2.0 μg/mL) for 3 h. a–e Partially enlarged view of **a**–**e**. The white scale bar in **a** represents 200 μm; the white dotted box in **a** is the enlarged image in the region; the white arrow in a indicates a typical ISV; the white dotted lines in b–e represent the dorsal edge of zebrafish. **f** Statistical analysis of the total length of ISVs in the treatment group over the total length of ISVs in the PTK787-treated group. Data are plotted as the mean ± SEM.*$P < 0.05$ vs. the PTK787- treated group

reduced wound width (76.7 ± 4.8% and 77.5 ± 9.9%), and treatment with 10 μM induced almost complete wound closure (96.2 ± 4.5%) at 24 h. In addition, Fig. 2c shows a 1.15-, 1.08-, 1.28-, and 1.67-fold increase in cell number after a 24-h incubation with 0.1, 0.5, 1, and 10 μM CA, respectively.

CA increased HUVEC migration

The ability of CA to stimulate endothelial migration was tested using Transwell plates. After a 24-h incubation with CA at different concentrations (0.1, 1, 5, and 10 μM), 22.8 ± 2.8, 28.2 ± 2.5, 35.6 ± 1.7, and 33.4 ± 2.4 cells per field migrated across the filer, respectively. The enhanced migration of HUVECs was concentration-dependent and reached a plateau at 5 and 10 μM CA (Fig. 2d, e).

CA enhanced HUVEC tube formation and rescued HUVEC tube damage

Matrigel is a reasonable proxy for in vivo tube formation. However, assessment of tube formation in the setting of sustained or chronic damage, as may be present in a chronic wound, is also valuable. The ability of endothelial cells to remodel and align is a requirement for the formation of new blood vessels during angiogenesis, and it can be tested by the in vitro tube formation assay. CA enhanced HUVEC tube-like structure formation after a 4-h incubation of HUVECs. Figure 3a, b demonstrated that CA at 10 μM enhanced HUVEC tube-like structure formation by approximately 35% compared with the control cells. In a 12-day tube formation assay using HUVECs seeded in a bed of fibroblasts, a preliminary screen of *C. Cassia* compounds supported CA's ability to rescue tube formation in the presence of homocysteine-induced damage (Fig. 3c, d).

CA elevated VEGF secretion

VEGF is a survival factor for endothelial cells, and its secretion may be actively involved in angiogenesis. In Supplementary Figure S2, the ELISA results showed a concentration- and time-dependent increase of VEGF secretion in the supernatants of HUVECs that have been treated with CA. When HUVECs were treated with increasing concentrations of CA (1, 5, and 10 μM), significantly higher levels of VEGF were detected after 48 h. The maximal effect, approximately a 3-fold increase compared with the control group, was observed for 10 μM CA (Figure S1A). When HUVECs were treated with 10 μM CA for 0, 24, 36, 48, and 72 h, the secretion of VEGF increased with time, reaching a maximal level at 48 h (Figure S1B).

CA activated PI3K/AKT and MAPK signaling pathways

To evaluate the effects of CA on PI3K/AKT and MAPK signaling pathways, western blot assays were performed. In the PI3K/AKT signaling pathway, phosphorylation of AKT and its downstream target eNOS were both induced in a dose-dependent-manner up to a peak at 10 μM CA (Fig. 4a, c). This activation was also time-dependent, as AKT and eNOS phosphorylation was detected as early as 5 min, peaked at 15–30 min, before falling at 60 and 120 min (Fig. 4b, d). In addition, for the MAPK signaling pathway, the phosphorylation of c-Raf and Erk increased at concentrations up to 10 μM

(Fig. 4e, g), whereas the phosphorylation of P38 maintained a plateau from 1 to 10 μM (Fig. 4i). CA treatment increased phosphorylation of c-Raf and its downstream target Erk at 5 min before reaching a maximum level at 30 and 60 min (Fig. 4f, h). P38, which is capable of improving endothelial cell motility [30], was initially phosphorylated 5 min after the CA treatment (Fig. 4j). To further determine whether the angiogenic activity of CA occurred through the AKT and Erk signaling pathways, we used LY294002 (a PI3K inhibitor) and U0126 (a MEK inhibitor). LY294002 reversed the phosphorylation of AKT, and U0126 blocked the phosphorylation of Erk (Fig. 5e, f). The stimulatory effects of CA on cell proliferation, VEGF secretion, and even tube formation were all decreased by LY294002 and U0126 pretreatment (Fig. 5a–d).

CA partially restored intersegmental vessels in zebrafish pretreated with PTK787

A transgenic zebrafish strain (vegfr2: GFP) was used to assess the angiogenic effects of CA. The formation of intersegmental vessels (ISVs) in these animals can be blocked with selective inhibitors of VEGFR tyrosine kinase, such as PTK787. Zebrafish embryos treated with 0.5–3.0 μg/mL PTK787 for 3 h demonstrated a dose-dependent reduction in ISV lengths (Supplementary Figure S3). Several off-target effects, such as pericardial edema and trunk flexion, were observed when zebrafish embryos were exposed to 3.0 μg/mL PTK787. Therefore, 2.0 μg/mL PTK787 was chosen to induce zebrafish ISV loss (Fig. 6b). Incubation of the PTK787-pretreated embryos with 0.01, 0.05, and 0.1 μg/mL CA for 24 h partially restored ISV formation (Fig. 6c–e). This dose-dependent recovery was confirmed by quantitative analysis of ISV lengths (Fig. 6f).

CA up-regulated angiogenesis in vivo

To investigate the in vivo activities of CA on angiogenesis, a mouse Matrigel plug assay was employed. Matrigel plugs that are treated with saline were pale in color, which demonstrates no or little blood vessel formation. Whereas compared with the saline controls, Matrigel plugs treated with CA appeared red in color, which indicates that CA promoted angiogenesis in vivo (Fig. 7a). The content of hemoglobin (Hb) inside the Matrigel plugs was measured to evaluate the pro-angiogenic effects of CA. As shown in Fig. 7b, the Hb level in saline control was almost 1.8 g/dL, and CA significantly elevated the Hb level to nearly 3.2 g/dL ($P < 0.05$). Compared with the saline group, Hematoxylin–eosin (HE) staining and CD31 immunohistochemistry illustrated more capillary-like structures and neovessels, and vascular wall thickening in the CA-treated group (Fig. 7c, d).

CA promoted wound healing in vivo

The effect of CA on wound healing was investigated in vivo. Daily intraperitoneal injection of CA (25, 50, and 100 mg/kg) markedly accelerated wound healing in wild-type (WT) (over 12 days) and diabetic (*db/db*) mice (over 16 days). From day 4 to day 10, the CA-treated wounds in WT mice were significantly smaller in size than in mice treated with physiological saline. On day 12 post-wounding, the untreated wounds achieved complete closure. In comparison, the CA treatment group (50 mg/kg) obtained earlier healing (on day 10) and exhibited 98.2 ± 2.5% wound closure, whereas only 89.0 ± 1.9% closure was observed in the 25 mg/kg CA treatment group and 79.8 ± 3.8% in the control group (Fig. 8a). Additionally, as shown in Fig. 8b, CA (25, 50 and 100 mg/kg) dose-dependently improved wound healing in diabetic mice, with complete closure after 16 days at 50 and 100 mg/kg CA, and only 82.9 ± 8.6% and 75.7 ± 2.4% closure was observed in mice treated with 25 mg/kg CA and physiological saline, respectively ($P < 0.05$). Our data demonstrated that the overall rate of wound healing in *db/db* mice was much slower than of WT mice. No significant reduction in body weight or blood glucose levels was observed after the administration of CA throughout the experiment (Supplementary Table S2–S4).

To further determine the effect of CA on wound contraction and closure, histological analyses were performed. HE staining showed that the WT and *db/db* mice treated with 50 mg/kg CA achieved complete epidermal regeneration and remodeling of the dermis on day 10 post-wounding, whereas the wounds in their corresponding control group were only partly closed at the same time point (Fig. 8c). Because angiogenesis plays a major role in wound healing, immunochemistry analysis was carried out using a monoclonal antibody against the endothelial cell marker CD31 to quantitate vascular density in the wound bed. On day 10 post-wounding, slightly higher levels of capillary density were detected in WT mice vs. *db/db* mice. After the administration of 50 mg/kg CA, significantly more capillaries were formed compared with physiological saline-treated mice ($P < 0.001$). In WT mice, 166 ± 8 vessels per field were detected in the CA-treated group compared with 56 ± 6 vessels per field in the control group. In *db/db* mice, there was a robust increase in capillary density in the wounds of CA-treated mice (151 ± 6 vessels per field) compared with physiological saline-treated mice (33 ± 4 vessels per field) (Fig. 8d).

VEGF is an important growth factor in wound healing because it promotes early events in angiogenesis, particularly endothelial cell migration and proliferation. To evaluate the efficacy of CA in up-regulating the expression of VEGF in vivo, a western blot assay was performed on tissue homogenate from the cutaneous wound edges. As shown in

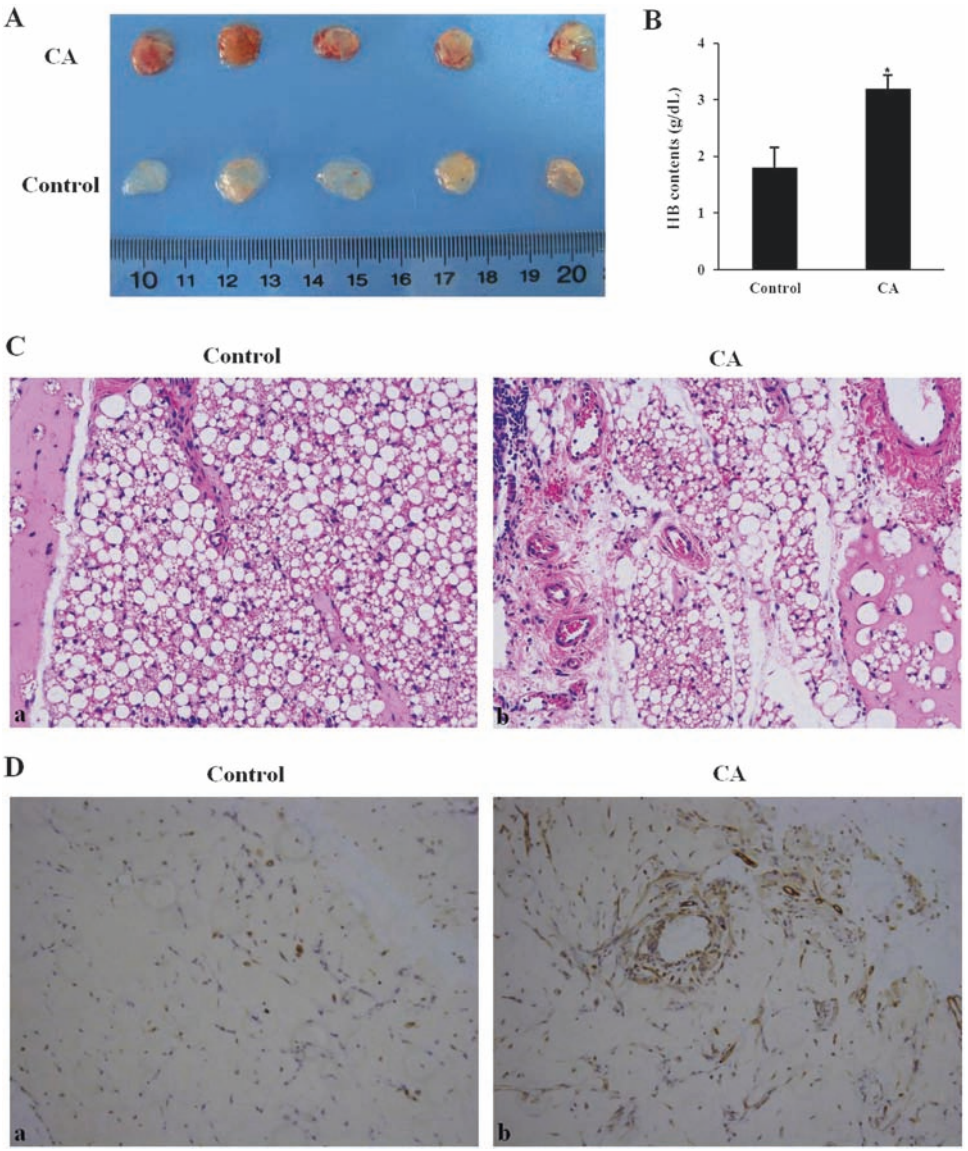

Fig. 7 Pro-angiogenic effect of CA (100 mg/kg) in the Matrigel plug assay. **a** Representative pictures of Matrigel plugs from the indicated groups at day 15 after inoculation into mice. **b** Hb content was measured from the implanted matrigel plugs in mice. The result was obtained from three individual experiments. Data shown in the graphs are representative of the mean ± SEM. $^{*}P < 0.05$ vs. vehicle control. **c** HE staining of Matrigel plugs in the control mice (**a**) and the CA-treated mice (**b**) (magnification ×200). **d** Immunohistochemical analysis of CD31 expression in the Matrigel plugs of the control mice (**a**) and the CA-treated mice (**b**) (magnification ×100; positive immunoreactivity appears brown)

Fig. 8e and f, VEGF protein was increased around the damaged tissues compared with the unwounded skin. Additionally, after the treatment with 50 mg/kg, the expression of VEGF was up-regulated by 1.6- and 3.1-fold in WT and *db/db* mice relative to the respective control groups ($P < 0.001$). This in vivo increase of VEGF can be due to an increased endothelial cell number in CA-treated wounds (Fig. 8d), because CA increases VEGF secretion by these endothelial cells, macrophages, keratinocytes, etc., which are already present in the lesion (Supplementary Figure S2), or due to a combination of the two reasons.

Discussion

Our data clearly showed that CA efficiently promoted endothelial cell proliferation, migration and tube formation that contributed to the process of neovessel formation. Furthermore, CA also induced the phosphorylation of AKT, Erk1/2, and P38, which are central signaling molecules during the process of angiogenesis. Considering that wound healing is delayed in diabetes due to aberrant angiogenesis, we used a full-thickness excision wound model to evaluate the pro-angiogenic effects of CA in vivo. In WT and *db/db* mice, CA stimulated angiogenesis and wound healing. Of particular relevance to our findings, here is a recent human clinical trial reporting that application of 2% cinnamon ointment on episiotomy incisions has a significant effect on decreasing perineal pain and accelerating healing of the incision [31]. Although these authors did not reveal the active substances in the cinnamon ointment, it was known that three main compounds in cinnamon, namely, CA, eugenol, and linalool, make up approximately 80% of its composition [32].

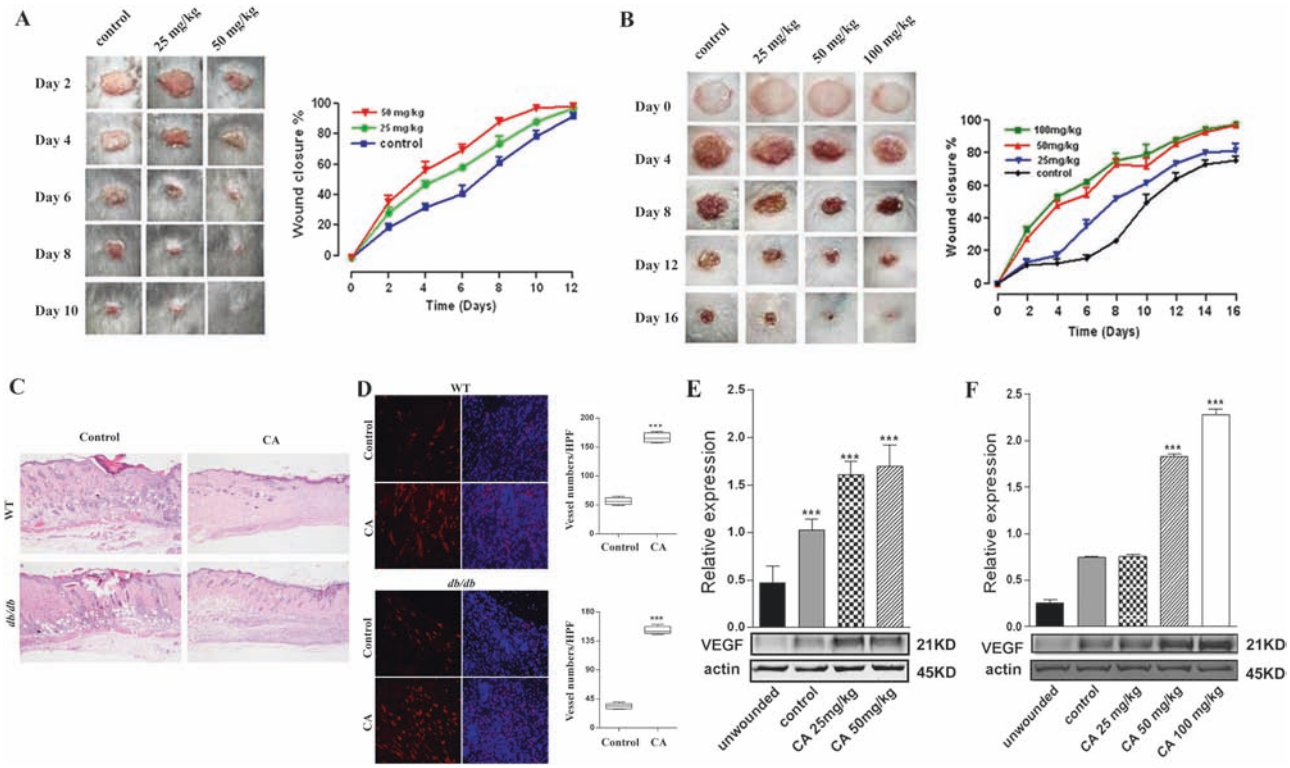

Fig. 8 CA induced wound healing in vivo. **a**, **b** Wild-type (WT, **a**) and wounded diabetic (*db/db*, **b**) mice were treated with CA or vehicle solution daily until wound closure. The representative photographs of the wounds (left) and overall rates of wound closure (right) in WT and *db/db* mice are shown. There was a significant acceleration of wound healing in the CA treatment group vs. the control group (ten mice in each group; $P < 0.05$). **c** HE staining of wounds from WT and *db/db* mice on day 10 post-wounding (magnification ×40). **d** Blood vessels were detected with an anti-CD31 antibody (red), and nuclei were counter-stained by DAPI (blue) (magnification ×200). Representative photomicrographs of wound vascularity were obtained on day 10 post-treatment with CA (50 mg/kg) and physiological saline in WT and *db/db* mice. The bar graphs represented an average of vessel density (the number of vessels per field) of five randomly selected fields from five independent mouse wounds. **e**, **f** CA induced VEGF expression around cutaneous wounds. Western blot was performed to measure VEGF expression. Tissue homogenates of wound edges were harvested from WT (**e**) and *db/db* (**f**) mice treated with CA for 10 days. Both the physiological saline-treated group and the unwound group were used as controls ($n = 5$/each group). Data shown in the graphs are representative of the mean ± SEM. $^{***}P < 0.001$ vs. the control

Angiogenesis involves a sequence of events that lead to the formation of new blood vessels from the pre-existing vascular network and play an essential role in wound healing [33]. Although topical administration of activated platelet supernatant or recombinant PDGF have been reported to improve diabetic foot ulcers, refractory wounds in diabetes are still a clinical problem, which can even result in amputation [34, 35]. *C. cassia*, a traditional folk herb, has been used for diabetes mellitus therapy and impaired wound healing treatment [20, 36–38]. CA is a major volatile oil purified from the bark of *C. cassia*, and oral administration of CA produced a hypoglycemic effect in streptozotocin-induced diabetic Wistar rats from day 28 onward [39–41]. Our data illustrated that time to wound closure was reduced by CA in WT and *db/db* mice. The optimal CA dose was 50 mg/kg, which was far less than 229.5 mg/kg (LD_{50} value reported by Huang et al. [42]). Of note is that in the *db/db* mice, no significant change was observed in blood glucose level during the experiment, which ended on day 16 when complete wound closure was almost achieved. This is consistent with the aforementioned studies, which showed that the hypoglycemic effect of CA began after 28 days of administration [41]. It appeared that in the current conditions, CA-induced wound healing was independent of reduced blood glucose.

Many endogenous growth factors, especially VEGF, are believed to be pivotal signaling molecules in angiogenesis during the process of wound healing [43]. VEGF is a potent stimulator of angiogenesis that directly induces endothelial cell proliferation and migration [44], and it is therefore important to study the VEGF signaling pathway as it relates to the acceleration of wound healing. A previous study had shown that *C. cassia* stimulated VEGF secretion in HUVECs (2-fold) and in bovine aortic endothelial cells (1.6-fold), compared with the controls [23]. Our current research demonstrated that CA induced VEGF secretion from HUVECs by three-fold. This suggests that CA may be one of the principal components of *C. cassia*

responsible for this effect. Based on our in vivo observations, follow-up studies using immunohistochemistry and western blot were performed at the optimal dose of 50 mg/kg. In skin wounds, we detected an increase of VEGF protein expression around the margin of wounded tissue. Furthermore, CD31-positive capillaries in the wound bed and surrounding tissues were also significantly increased, which further supported the effect of CA on angiogenesis during wound healing. These findings demonstrated that the pro-angiogenic effects of CA were associated with increased expression of VEGF. In contrast to our present results, Lu et al. [45] showed that a water-based extract from cinnamon inhibited VEGF-induced endothelial cell proliferation, migration, and tube formation in vitro, sprout formation from aortic ring ex vivo and tumor-induced blood vessel formation in vivo. CA, a component responsible for the aroma of cinnamon, had little inhibitory effect on VEGFR-2 kinase activity. Whereas the high-performance liquid chromatography-purified components of cinnamon, including type A trimeric and tetrameric procyanidins, were found to inhibit kinase activity of purified VEGFR-2 and VEGFR-2 signaling, implicating oligomeric procyanidins as active components in cinnamon that inhibited angiogenesis. It is noteworthy that the CA derivative 2-methoxycinnamaldehyde has been shown to inhibit tumor angiogenesis by suppressing Tie2 activation [46], while the CA derivative CB403 exerted its antitumor effect through the arrest of cell cycle progression in the G2/M phase [47]. As previously reported, a single medicinal plant may contain both pro- and anti-angiogenic compounds [48, 49]. Taken together, these findings emphasize the need for regulations that standardize herbal therapy, which is currently under the US Dietary Supplement and Health Education Act. It is also clear that pure phytochemicals with defined pharmacological profile are much safer and reliable than crude extracts for clinical uses.

Erk1/2 is one of the major molecules of the MAPK signaling pathway, which is activated through the three-component protein kinase cascade Raf → MEK → Erk [50]. The Raf/MEK/Erk signaling pathway is well recognized to be involved in cell proliferation and plays a critical role in promoting angiogenesis during wound healing [51, 52]. The present finding suggested that CA induced both the phosphorylation of Erk and angiogenesis by HUVECs, which was blocked by U0126 (a MEK inhibitor). P38 MAPK signaling can act as a "molecular switch" between angiogenesis and hyper-permeability, improving endothelial cell motility [30]. The phosphorylation of P38 was found to be induced by CA in a time- and concentration-dependent manner in our study. In a previous study, P38 and Erk1/2 were activated and phosphorylated by CA at 1 μM for 24 h in PLC/PRF/5 cells, but cell proliferation was inhibited [53]. In contrast, our study demonstrated that proliferation of HUVECs was stimulated after a 24-h incubation with 10 μM CA. These contrasting results may be due to the differences in cell type, drug concentration, and medium conditions. Another central pathway that controls the process of angiogenesis in endothelial cells is the PI3K/AKT signaling pathway [54]. Phosphorylation of AKT subsequently activates eNOS at serine1177, which leads to the production of NO, which can simulate vasodilation, vascular remodeling and angiogenesis [55, 56]. Our findings demonstrate that CA stimulates AKT activation, and the effect is blocked by LY194002 (a PI3K inhibitor). It is important to comment further on the effect of CA on eNOS and other members of the extremely diverse NOS family. CA had been shown in a variety of settings to down-regulate inducible nitric oxide synthase (iNOS) and NO release, in lipopolysaccharide-stimulated macrophages in vitro at concentrations as low as 5 μM [57, 58]. Unlike eNOS, iNOS produces large amounts of NO as part of an immune response, and it may contribute in a small way to VEGF-induced vascular permeability and angiogenesis [59], iNOS activation or expression is strongly associated with a host of tissue-destructive processes such as chronic inflammatory and autoimmune diseases [58]. Inhibition of iNOS can conceivably protect the vasculature from further inflammatory damage in the chronic wound setting. In our study, we observed CA induced phosphorylation of eNOS in a dose-dependent manner. The prospect of a small molecule, such as CA, that can up-regulate eNOS but also down-regulate iNOS in an inflammatory setting is intriguing and warrants further investigation.

In summary, we demonstrated that CA accelerated wound healing in vitro and in vivo by inducing angiogenic activity. This was evidenced in both zebrafish and murine models. The potential mechanism involved enhancing secretion of VEGF and activating both the PI3K/AKT and MAPK signaling pathways. These results underscored the pro-angiogenic effects of CA, and like ginsenoside Rg1 [48] and salvianolic acid A [60], CA can be a prototype for non-peptide molecules that can induce therapeutic angiogenesis, as in chronic diabetic wounds and myocardial infarction.

Acknowledgements The work was supported by program NCET Foundation, NSFC (81602980, 81473327, 81230090), partially supported by Global Research Network for Medicinal Plants (GRNMP), King Saud University, Shanghai Leading Academic Discipline Project (B906), Key laboratory of drug research for special environments, PLA, Shanghai Engineering Research Center for the Preparation of Bioactive Natural Products (10DZ2251300), the Scientific Foundation of Shanghai China (12401900801, 13401900101), National Major Project of China (2011ZX09307-002-03), the National Key Technology R&D Program of China (2012BAI29B06), and a grant to Department of Pharmacology, University of Cambridge by Shanghai Hutchison Pharmaceuticals Limited.

Compliance with Ethical Standards

Conflict of interest The authors declare that they have no conflict of interest.

References

1. Jeffcoate WJ, Harding KG. Diabetic foot ulcers. Lancet. 2003;361:1545–51.
2. Fonder MA, Lazarus GS, Cowan DA, et al. Treating the chronic wound: a practical approach to the care of nonhealing wounds and wound care dressings. J Am Acad Dermatol. 2008;58:185–206.
3. Tonnesen MG, Feng X, Clark RA. Angiogenesis in wound healing. J Invest Dermatol Symp Proc. 2000;5:40–46.
4. Robinson MJ, Cobb MH. Mitogen-activated protein kinase pathways. Curr Opin Cell Boil. 1997;9:180–6.
5. Shiojima I, Walsh K. Role of Akt signaling in vascular homeostasis and angiogenesis. Circ Res. 2002;90:1243–50.
6. Berra E, Milanini J, Richard DE, et al. Signaling angiogenesis via p42/p44 MAP kinase and hypoxia. Biochem Pharmacol. 2000;60:1171–8.
7. Johnson GL, Lapadat R. Mitogen-activated protein kinase pathways mediated by ERK, JNK, and p38 protein kinases. Science. 2002;298:1911–2.
8. Manning BD, Cantley LC. AKT/PKB signaling: navigating downstream. Cell. 2007;129:1261–74.
9. Papanas N, Maltezos E. Growth factors in the treatment of diabetic foot ulcers: new technologies, any promises? Int J Low Extrem Wounds. 2007;6:37–53.
10. Papanas N, Maltezos E. Becaplermin gel in the treatment of diabetic neuropathic foot ulcers. Clin Interv Aging. 2008;3:233–40.
11. FDA. Communication about an Ongoing Safety Review Regranex (becaplermin) (2008). http://www.fda.gov.
12. Majewska I, Gendaszewska-Darmach E. Proangiogenic activity of plant extracts in accelerating wound healing-a new face of old phytomedicines. Acta Biochim Pol. 2011;58:449–60.
13. Fan TP, Yeh JC, Leung KW, et al. Angiogenesis: from plants to blood vessels. Trends Pharmacol Sci. 2006;27:297–309.
14. Ranasinghe P, Pigera S, Premakumara GA, et al. Medicinal properties of 'true'cinnamon (Cinnamomum zeylanicum): a systematic review. BMC Complement Altern Med. 2013;13:275.
15. Commission CP. Chinese pharmacopoeia. Vol. 328. Beijing: Chemical Industry Press; 2005. p. 547.
16. Kim SY, Koo YK, Koo JY, et al. Platelet anti-aggregation activities of compounds from *Cinnamomum cassia*. J Med Food. 2010;13:1069–74.
17. Plaisier C, Cok A, Scott J, et al. Effects of cinnamaldehyde on the glucose transport activity of GLUT1. Biochimie. 2011;93:339–44.
18. Schmidt E, Jirovetz L, Buchbauer G, et al. Composition and antioxidant activities of the essential oil of cinnamon (Cinnamomum zeylanicum Blume) leaves from Sri Lanka. J Essent Oil Bear Plants. 2006;9:170–82.
19. Lee HS, Ahn YJ. Growth-inhibiting effects of *Cinnamomum cassia* bark-derived materials on human intestinal bacteria. J Agric Food Chem. 1998;46:8–12.
20. Kim SH, Hyun SH, Choung SY. Anti-diabetic effect of cinnamon extract on blood glucose in db/db mice. J Ethnopharmacol. 2006;104:119–23.
21. Kamath JV, Rana AC, Chowdhury AR. Pro-healing effect of Cinnamomum zeylanicum bark. Phytother Res. 2003;17:970–2.
22. Farahpour MR, Habibi M. Evaluation of the wound healing activity of an ethanolic extract of Ceylon cinnamon in mice. Vet Med. 2012;57:53–57.
23. Choi DY, Baek YH, Huh JE, et al. Stimulatory effect of *Cinnamomum cassia* and cinnamic acid on angiogenesis through up-regulation of VEGF and Flk-1/KDR expression. Int Immunopharmacol. 2009;9:959–67.
24. Yu R, Sheng MP, Jiang WD. Effects of Shexiang Baoxin Wan in a rabbit model of acute myocardial infarction. Chin J New Drugs Clin Remedies. 2001;20:1–3.
25. Wang SS, Yong L, Fan WH. Angiogenesis promoting effect of Shexiang Baoxin Pill on chicken embryo chorioallantoic membrane and cultured microvuscular endothelial cells. Chinese. J Integr Tradit West Med. 2003;23:128–31.
26. Song HT, Guo T, Zhao MH, et al. Pharmacodynamic studies on heart-protecting musk pills with myocardial blood flow perfusion in rats. Pharm J Chin People's Lib Army. 2002;18:137–40.
27. Senanayake UM, Lee TH, Wills RBH. Volatile constituents of cinnamon (Cinnamomum zeylanicum) oils. J Agric Food Chem. 2002;26:822–4.
28. Wake H, Mori S, Liu K, et al. Histidine-rich glycoprotein inhibited high mobility group box 1 in complex with heparin-induced angiogenesis in matrigel plug assay. Eur J Pharmacol. 2009;623:89–95.
29. Ehanire T, Ren L, Bond J, et al. Angiotensin II stimulates canonical TGFβ signaling pathway through angiotensin receptor 1 to induce granulation tissue contraction. J Mol Med (Berl). 2015;93:289–302.
30. Issbrücker K, Marti HH, Hippenstiel S, et al. p38 MAP kinase-a molecular switch between VEGF-induced angiogenesis and vascular hyperpermeability. FASEB J. 2003;17:262–4.
31. Mohammadi A, Mohammad-Alizadeh-Charandabi S, Mirghafourvand M, et al. Effects of cinnamon on perineal pain and healing of episiotomy: a randomized placebo-controlled trial. J Integr Med. 2014;12:359–66.
32. Chericoni S, Prieto JM, Iacopini P, et al. In vitro activity of the essential oil of Cinnamomum zeylanicum and eugenol in peroxynitrite-induced oxidative processes. J Agric Food Chem. 2005;53:4762–5.
33. Madeddu P. Therapeutic angiogenesis and vasculogenesis for tissue regeneration. Exp Physiol. 2005;90:315–26.
34. Steed DL, Goslen JB, Holloway GA, et al. Randomized prospective double-blind trial in healing chronic diabetic foot ulcers: CT-102 activated platelet supernatant, topical versus placebo. Diabetes Care. 1992;15:1598–604.
35. Steed DL. Clinical evaluation of recombinant human platelet–derived growth factor for the treatment of lower extremity diabetic ulcers. Diabetic Ulcer Study Group. J Vasc Surg. 1995;21:71–81.
36. Khan A, Safdar M, Ali Khan MM, et al. Cinnamon improves glucose and lipids of people with type 2 diabetes. Diabetes care. 2003;26:3215–8.
37. Ulbricht C, Seamon E, Windsor RC, et al. An evidence-based systematic review of cinnamon (Cinnamomum spp.) by the Natural Standard Research Collaboration. J Diet Suppl. 2011;8:378–454.
38. Dugoua JJ, Seely D, Perri D, et al. From type 2 diabetes to antioxidant activity: a systematic review of the safety and efficacy of common and cassia cinnamon bark. Can J Physiol Pharmacol. 2007;85:837–47.
39. Zhang W, Xu YC, Guo FJ, et al. Anti-diabetic effects of cinnamaldehyde and berberine and their impacts on retinol-binding protein 4 expression in rats with type 2 diabetes mellitus. Chin Med J. 2008;121:2124–8.
40. Babu PS, Prabuseenivasan S, Ignacimuthu S. Cinnamaldehyde-a potential antidiabetic agent. Phytomedicine Int J Phytother Phytopharm. 2007;14:15–22.
41. Zheng H, Whitman SA, Wu W, et al. Therapeutic potential of Nrf2 activators in streptozotocin-induced diabetic nephropathy. Diabetes. 2011;60:3055–66.

42. Huang J, Wang S, Luo X, et al. Cinnamaldehyde reduction of platelet aggregation and thrombosis in rodents. Thromb Res. 2007;119:337–42.
43. Barrientos S, Stojadinovic O, Golinko MS, et al. Growth factors and cytokines in wound healing. Wound Repair Regen. 2008;16:585–601.
44. Breen EC. VEGF in biological control. J Cell Biochem. 2007;102:1358–67.
45. Lu J, Zhang K, Nam S, et al. Novel angiogenesis inhibitory activity in cinnamon extract blocks VEGFR2 kinase and downstream signaling. Carcinogenesis. 2010;31:481–8.
46. Yamakawa D, Kidoya H, Sakimoto S, et al. 2-Methoxycinnamaldehyde inhibits tumor angiogenesis by suppressing Tie2 activation. Biochem Biophys Res Commun. 2011;415:174–80.
47. Jeong HW, Han DC, Son KH, et al. Antitumor effect of the cinnamaldehyde derivative CB403 through the arrest of cell cycle progression in the G2/M phase. Biochem Pharmacol. 2003;65:1343–50.
48. Sengupta S, Toh SA, Sellers LA, et al. Modulating angiogenesis the Yin and the Yang in ginseng. Circulation. 2004;110:1219–25.
49. Yeh JC, Cindrova-Davies T, Belleri M, et al. The natural compound n-butylidenephthalide derived from the volatile oil of Radix Angelica sinensis inhibits angiogenesis in vitro and in vivo. Angiogenesis. 2011;14:187–97.
50. Pang X, Yi T, Yi Z, et al. Morelloflavone, a biflavonoid, inhibits tumor angiogenesis by targeting rho GTPases and extracellular signal-regulated kinase signaling pathways. Cancer Res. 2009;69:518–25.
51. Chim SM, Qin A, Tickner J, et al. EGFL6 promotes endothelial cell migration and angiogenesis through the activation of extracellular signal-regulated kinase. J Biol Chem. 2011;286:22035–46.
52. Kim WS, Yang YJ, Min HG, et al. Accelerated wound healing by S-methylmethionine sulfonium: evidence of dermal fibroblast activation via the ERK1/2 pathway. Pharmacology. 2010;85:68–76.
53. Wu SJ, Ng LT, Lin CC. Cinnamaldehyde-induced apoptosis in human PLC/PRF/5 cells through activation of the proapoptotic Bcl-2 family proteins and MAPK pathway. Life Sci. 2005;77:938–51.
54. Somanath PR, Razorenova OV, Chen J, et al. Akt1 in endothelial cell and angiogenesis. Cell Cycle. 2006;5:512–8.
55. Dimmeler S, Fleming I, Fisslthaler B, et al. Activation of nitric oxide synthase in endothelial cells by Akt-dependent phosphorylation. Nature. 1999;399:601–5.
56. Fulton D, Gratton JP, McCabe TJ, et al. Regulation of endothelium-derived nitric oxide production by the protein kinase Akt. Nature. 1999;399:597–601.
57. Kim DH, Kim CH, Kim MS, et al. Suppression of age-related inflammatory NF-κB activation by cinnamaldehyde. Biogerontology. 2007;8:545–54.
58. Liao JC, Deng JS, Chiu CS, et al. Anti-inflammatory activities of Cinnamomum cassia constituents in vitro and in vivo. Evid Based Complement Alternat Med. 2012. https://doi.org/10.1155/2012/429320.
59. Fukumura D, Gohongi T, Kadambi A, et al. Predominant role of endothelial nitric oxide synthase in vascular endothelial growth factor-induced angiogenesis and vascular permeability. Proc Natl Acad Sci. 2001;98:2604–9.
60. Li YJ, Duan CL, Liu JX. Salvianolic acid A promotes the acceleration of neovascularization in the ischemic rat myocardium and the functions of endothelial progenitor cells. J Ethnopharmacol. 2014;151:218–27.